Mapping Electron Transfer Pathways in a Chromophore−Quencher Triad

Joseph A. Treadway,[†] Pingyun Chen,[†] Todd J. Rutherford,[‡] F. Richard Keene,[‡] and Thomas J. Meyer*,[†]

Department of Chemistry, The University of North Carolina CB#3290,
Chapel Hill, North Carolina 27599-3290, and Department of Chemistry and Chemical Engineering,
James Cook University of North Queensland, Townsville, Queensland 4811, Australia

Received: May 16, 1997; In Final Form: July 10, 1997[⊗]

A comparative study of the photophysics of the four positional isomers (one *trans* and three *cis*) of the chromophore−quencher triad [Ru^{II}(dmb)(bpyCH$_2$PTZ)(bpyCH$_2$MV^{2+})]$^{4+}$ (dmb is 4,4′-dimethyl-2,2′-bipyridine, bpyCH$_2$PTZ is (4′-methyl-4-(2,2′-bipyridin-4-yl)methyl)phenothiazine, and bpyCH$_2$MV^{2+} is (4′-methyl-4-(2,2′-bipyridin-4-yl)methyl)-1′-methyl-4,4′-bipyridinium cation) has been undertaken. Following metal-to-ligand charge transfer (MLCT) excitation by laser flash photolysis at 460 or 532 nm, the redox-separated states [Ru^{II}(dmb)(bpyCH$_2$PTZ$^{\bullet+}$)(bpyCH$_2$MV$^{\bullet+}$)]$^{4+}$ are formed rapidly (< 5 ns). Quenching of MLCT emission occurs with near unit efficiency for all four isomers. For the *trans* and *cis3* isomers, formation of the redox-separated state is ~25% efficient. For back electron transfer from −MV$^+$ to −PTZ$^+$, $\Delta G^0 = -1.14$ eV for all four isomers from electrochemical measurements and yet k_{ET} varies from 4.5×10^6 to 8.7×10^6 s^{-1} in acetonitrile at 25 °C.

The coordination of unsymmetrically-substituted bidentate ligands to an octahedral center such as ruthenium(II) gives rise to stereoisomerism based on the relative positions of the substituents. Such geometrical isomerism, positional isomerism, has been recognized in the past, but little was known about what effect it might have on chemical and physical properties since there was no means for obtaining isomerically pure samples.[1] For instance, Opperman *et al.*[2] prepared a series of Ru(II) polypyridyl complexes containing linked phenothiazine electron transfer donors and anthraquinone acceptors. Although it was recognized that the chromophore−quencher existed in different isomeric forms, it was not possible to discern whether or not all of the four possible isomers were present in the sample and, therefore, if electron transfer kinetics observed following laser flash photolysis were of a single isomer or an average. This issue has been raised by others as well.[3] Positional isomerism is illustrated in Figure 1 for the four isomers of the chromophore−quencher complex [Ru^{II}(dmb)(bpyCH$_2$PTZ)(bpyCH$_2$-MV^{2+})]$^{4+}$ **(1)** in which dmb is 4,4′-dimethyl-2,2′-bipyridine, bpyCH$_2$PTZ is (4′-methyl-4-(2,2′-bipyridin-4-yl)methyl)phenothiazine, and bpyCH$_2$MV^{2+} is (4′-methyl-4-(2,2′-bipyridin-4-yl)methyl)-1′-methyl-4,4′-bipyridinium cation.[4] We report here the development of techniques for the separation of these isomers and their use in mapping the various electron transfer pathways that they provide.

The synthesis of the target chromophore−quencher complex was based on a synthetic strategy for tris(heteroleptic) complexes reported previously[5] and is described in detail elsewhere.[6] It involves stepwise addition first of dmb to [Ru(CO)$_2$Cl$_2$]$_n$ to give [Ru(dmb)(CO)$_2$Cl$_2$], followed by bpyCH$_2$MV^{2+} and pyridine to give [Ru(dmb)(bpyCH$_2$MV^{2+})(py)$_2$]$^{4+}$ as the hexafluorophosphate salt. The two isomers of this complex (in which the MV^{2+} as a substituent is *trans* to one pyridine or *cis* to both) were separated by cation exchange chromatography (SP-Sephadex C25; aqueous sodium 4-toluenesulfonate eluent) by using a previously developed method.[7] The pyridyl ligands were displaced in refluxing ethylene glycol with an excess of bpyCH$_2$PTZ, which gave separate sets of the binary mixtures of geometrical isomers **1a**/**1b** and **1c**/**1d** with the stereochemistry from the first separation maintained.[8] These isomeric mixtures were also separated by cation exchange chromatography by utilizing aqueous sodium 4-toluenesulfonate as eluent. Precipitation from water with KPF$_6$ (2×) led to the isolation of pure PF$_6$$^-$ salts of the one *trans* and three *cis* isomers. The structures of **1a**, **1b**, **1c**, and **1d** were established by ^{1}H-NMR spectroscopy by utilizing ^{1}H COSY, as well as homonuclear decoupling and NOE measurements.[6] Extensive use was made

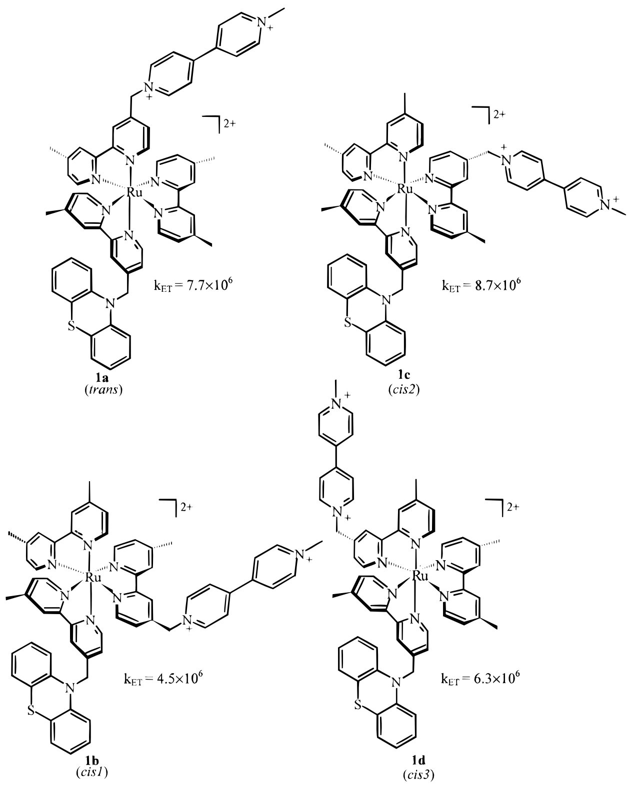

Figure 1. Geometrical isomers for [Ru^{II}(dmb)(bpyCH$_2$PTZ)(bpyCH$_2$-MV^{2+})]$^{4+}$ **(1)** with rate constants for back electron transfer (k_{ET}); see text. Each of these isomers exists as a pair of Δ/Λ enatiomers.

[†] The University of North Carolina.

[‡] James Cook University of North Queensland.

[⊗] Abstract published in *Advance ACS Abstracts,* August 15, 1997.

S1089-5639(97)01638-1 CCC: $14.00

SCHEME 1[a]

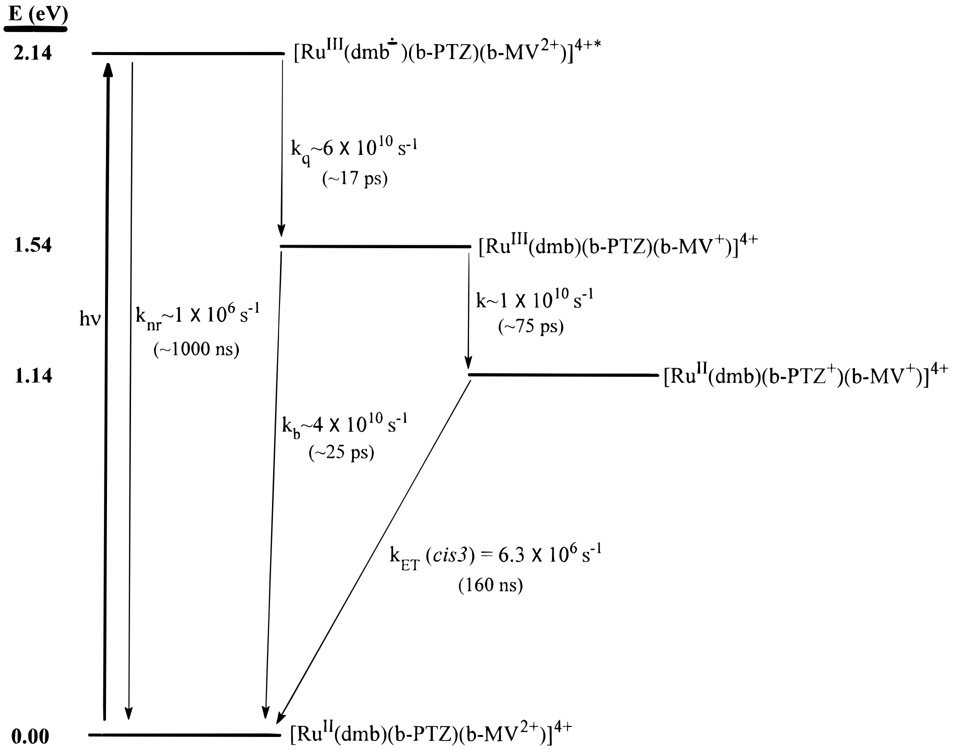

[a] In acetonitrile, b-MV^{2+} is $bpyCH_2MV^{2+}$, b-PTZ is $bpyCH_2PTZ$.

of the anisotropic interactions caused by differing degrees of shielding provided by the ring currents in differently substituted pyridyl rings as described previously.[9]

UV−visible absorption spectra of the four isomers are identical with an MLCT absorption band in acetonitrile appearing at $\lambda_{max} = 460$ nm ($\epsilon = 18\,600$ cm^{-1} M^{-1}), which is the λ_{max} for $[Ru(dmb)_3]^{2+}$. In cyclic voltammograms in acetonitrile 0.1 M in $[(n\text{-}C_4H_9)_4N]PF_6$ versus SSCE, waves appear for the couples $Ru^{III/II}$ ($E_{1/2} = +1.22$ V), $-PTZ^{+/0}$ ($E_{1/2} = 0.80$ V), $-MV^{2+/+}$ ($E_{1/2} = -0.34$ V), and $MV^{+/0}$ ($E_{1/2} = -0.74$ V). Polypyridyl-based reductions appeared at −1.37 and −1.57 V.

$$\begin{aligned} &[\mathrm{Ru^{III}(dmb^{\bullet-})(bpyCH_2PTZ)(bpyCH_2MV^{2+})}]^{4+}* \\ \mathbf{1} \xrightarrow{h\nu} &[\mathrm{Ru^{III}(dmb)(bpy^{\bullet-}CH_2PTZ)(bpyCH_2MV^{2+})}]^{4+}* \to \to \\ &[\mathrm{Ru^{III}(dmb)(bpyCH_2PTZ)(bpy^{\bullet-}CH_2MV^{2+})}]^{4+}* \\ &\underset{\mathbf{2}}{[\mathrm{Ru^{II}(dmb)(bpyCH_2PTZ^{\bullet+})(bpyCH_2MV^{\bullet+})}]^{4+}} \xrightarrow{k_{ET}} \mathbf{1} \end{aligned} \tag{1}$$

Compared to $[Ru(dmb)_3]^{2+}$ with an emission quantum yield of $\phi_{em} = 0.060$ in acetonitrile at 25° ± 2 °C, MLCT emission from **1** is >95% quenched and short on the ∼5 ns time scale.[10] Laser flash excitation at 460 or 532 nm (2.0−4.5 mJ/pulse) with absorbance monitoring from 350−700 nm under the same conditions with an apparatus described elsewhere[11] resulted in the <5 ns loss of the MLCT absorption at 460 nm, no evidence for the characteristic MLCT bleach at 460 nm, and the appearance of bands at $\lambda_{max} = 517$ nm[12] for $-PTZ^{\bullet+}$ and $\lambda_{max} = 397$ and 610 nm[13] for $-MV^{\bullet+}$ at the earliest observation times (∼5 ns). These observations are consistent with initial MLCT excitation followed by a series of rapid electron transfers to give redox-separated state, **2**, in eq 1. The quantum yields for appearance of **2** for the *trans* and *cis3* isomers (η_{rss}), Table 1, were measured relative to the efficiency of reaction 2.[14] Back electron transfer ($-MV^{\bullet+} \to -PTZ^{\bullet+}$), k_{ET} in eq 1, was studied by transient absorption measurements throughout the visible region from 350 to 690 nm. The results are summarized in Table 1. In all cases the variation in k_{ET} with observation wavelength was <3%, and the values in the table represent an average of measurements at 10−65 wavelengths.[15]

TABLE 1: $k_{ET}(\tau)$ and Efficiencies (η_{rss}) for Intramolecular Redox Separation in Deaerated Acetonitrile at 25° ± 2 °C

isomer	*trans* (**1a**)	*cis 1* (**1b**)	*cis 2* (**1c**)	*cis 3* (**1d**)
$k_{ET} \times 10^6$ s^{-1} [a]	7.7 (130 ns)[b]	4.5 (220 ns)	8.7 (115 ns)	6.3 (160 ns)
η_{rss}	0.20, 0.22, 0.25[c]			0.25

[a] Values reproducible to ±3%. [b] Weighted average of biexponential fits or best fit to exponential decay (ref 15). [c] Measured at concentrations of 3.4×10^{-6}, 2.4×10^{-5}, and 6.5×10^{-5} M, respectively, ±0.05. The slight variation in η_{rss} may be real but is within the experimental error.

$$[Ru(bpy)_3]^{2+}* + PTZ \to [Ru(bpy)_3]^{+} + PTZ^{\bullet+} \tag{2}$$

The kinetic scheme for formation of **2** is shown in Scheme 1. The first step is expected to be electron transfer to $-MV^{2+}$. On the basis of picosecond transient absorbance measurements in acetonitrile at 23 °C, Yonemoto *et al.*[16] concluded that MLCT excitation in $[Ru^{II}(bpy)_2(bpyCH_2MV^{2+})]^{4+}$ is followed by $bpy^{\bullet-} \to -MV^{2+}$ electron transfer to give $[Ru^{III}(bpy)_2(bpyCH_2MV^{\bullet+})]^{4+}$ with $k_q = 5.9 \times 10^{10}$ s^{-1} ($\tau = 17$ ps) and that back electron transfer to give the ground state occurs with $k_b = 4.0 \times 10^{10}$ s^{-1} ($\tau = 25$ ps). If the initial MLCT excited state(s) is reached with unit efficiency, $\eta_{rss} = k/(k + k_b)$ and if the rate constants measured by Yonemoto *et al.* are comparable in the *trans* and *cis3* isomers, k for $-PTZ \to Ru^{III}$ electron transfer is $\sim 1.3 \times 10^{10}$ s^{-1} ($\tau = 75$ ps).

Initial electron transfer from −PTZ to $Ru^{III}*$ is slow. In the model $[Ru^{II}(dmb)_2(bpy\text{-}CH_2PTZ)]^{2+}$, reductive quenching, eq 3, is uphill thermodynamically by ∼0.1 eV[17] and quenching is only partly complete as shown by the decrease in the luminescence quantum yield compared to $[Ru(dmb)_3]^{2+}*$ ($\phi_{em} = 0.044$

compared to $\phi_{em} = 0.060$) and a decrease in MLCT excited state lifetime from 900 to 680 ns.

$$[\mathrm{Ru^{III}(dmb^{\bullet -})(dmb)(bpyCH_2PTZ)}]^{2+*} \rightarrow [\mathrm{Ru^{II}(dmb^{\bullet -})(dmb)(bpyCH_2PTZ^{\bullet +})}]^{2+} \quad (3)$$

The data for k_{ET} in Table 1 map four distinct pathways for back electron transfer in the isomeric series. From the electrochemical measurements, $\Delta G^0 = -1.14$ eV for all four isomers, but k_{ET} varies from 4.5×10^6 to 8.7×10^6 s^{-1}. This is an important finding for earlier results on related systems where there were unresolved mixtures of isomers and, in retrospect, k_{ET} values were most likely averaged quantities for a series of isomers and not for a single isomeric assembly.

Given the known self-exchange rate constants for couples related to $-\mathrm{PTZ}^{+/0}$ and $-\mathrm{MV}^{2+/+}$, back electron transfer occurs in the inverted region since $\lambda \sim 0.9$ eV.[18] These reactions are remarkably slow given the small energy gap of 1.14 eV.[11] This must be a consequence of weak electronic coupling through the extended bond system at least for the *trans* isomer where, on the basis of molecular modeling,[19] the closest distance of through space $-\mathrm{MV}^{\bullet +}/-\mathrm{PTZ}^{\bullet +}$ approach is 16.5 Å (center to center). For the *cis* isomers there are accessible rotamers that bring them into edge to edge contact (7.0 Å center to center). The solvent and vibrational barriers to electron transfer for the *cis* isomers should be nearly the same. The differences in k_{ET} probably reflect differences in electronic coupling for them and subtle differences in their orbital pathways for electron transfer.

Acknowledgment. Financial support from the Australian Research Council and the U.S. National Science Foundation (Grant CHE-9321413) is gratefully acknowledged. Travel between the laboratories at JCUNQ and UNC (JAT and TJR) has been supported by the U.S. National Science Foundation (Grant INT-9015262) and the Australian Department of Industry, Science, and Technology and Tourism within the Australia-US Bilateral Science and Technology Program.

References and Notes

(1) Keene, F. R. *Coord. Chem. Rev.*, in press.

(2) Opperman, K. A.; Mecklenburg, S. L.; Meyer, T. J. *Inorg. Chem.* **1994**, *33*, 5295.

(3) Larson, S. L.; Elliott, C. M.; Kelley, D. F. *J. Phys. Chem.* **1995**, *99*, 6530.

(4) For each positional isomer there is a Δ, Λ enantiomeric pair. Each separate Λ "isomer" illustrated in Figure 1 has a corresponding Δ isomer present in equal amount in the isolated samples.

(5) (a) Anderson, P. A.; Deacon, G. B.; Haarmann, K. H.; Keene, F. R.; Meyer, T. J.; Reitsma, D. A.; Skelton, B. W.; Strouse, G. F.; Thomas, N. C.; Treadway, J. A.; White, A. H. *Inorg. Chem.* **1995**, *34*, 6145. (b) Strouse, G. F.; Anderson, P. A.; Schoonover, J. R.; Meyer, T. J.; Keene, F. R. *Inorg. Chem.* **1992**, *31*, 3004. (c) Anderson, P. A.; Strouse, G. F.; Treadway, J. A.; Keene, F. R.; Meyer, T. J. *Inorg. Chem.* **1994**, *33*, 3863.

(6) Rutherford, T. J.; Keene, F. R. *Inorg. Chem.* **1997**, *36*, 2872.

(7) (a) Rutherford, T. J.; Quagliotto, M. G.; Keene, F. R. *Inorg. Chem.* **1995**, *34*, 3857. (b) Rutherford, T. J.; Reitsma, D. A.; Keene, F. R. *J. Chem. Soc., Dalton Trans.* **1994**, 3659.

(8) Hua, X.; von Zelewsky, A. *Inorg. Chem.* **1995**, *34*, 5791.

(9) Rutherford, T. J.; Reitsma, D. A.; Keene, F. R. *J. Chem. Soc., Dalton Trans.* **1994**, 3659.

(10) There is evidence in the emission decay data for a small contribution (<3%) from an emissive impurity with $\tau \sim 1$ μs.

(11) (a) Chen, P.; Duesing. R.; Graff, D. K.; Meyer T. J. *J. Phys. Chem.* **1991**, *95*, 5850. (b) Duesing, R.; Tapolsky, G.; Meyer, T. J. *J. Am. Chem. Soc.* **1990**, *112*, 5378.

(12) Hester, R. E.; Williams, K. P. J. *J. Chem. Soc., Perkin Trans. 2* **1981**, 852.

(13) Watanabe, T.; Honda, K. *J. Phys. Chem.* **1982**, *86*, 2617.

(14) (a) The yield of $[\mathrm{Ru(bpy)_3}]^+$ and PTZ^+ following reductive quenching of $[\mathrm{Ru(bpy)_3}]^{2+*}$ by PTZ is ~1.0 relative to the $[\mathrm{Ru(bpy)_3}]^{2+} + \mathrm{MV}^{2+}$ actinometer in water (refs 14b,c). The measurements were made by measuring transient absorption changes at 10 wavelengths between 500 and 640 nm and known extinction coefficients with sufficient PTZ added (38 mM) to achieve >98% quenching. (b) Hoffman, M. Z. *J. Phys. Chem.* **1988**, *92*, 3458. (c) Hoffman, M. Z. *J. Phys. Chem.* **1991**, *95*, 2606.

(15) Kinetic decay of the *trans* form of **2** derived from **1a** is exponential with monitoring at 600−690 nm ($\lambda_{max} = 610$ nm for $-\mathrm{MV}^{\bullet +}$). The decay kinetics are better fit as biexponentials from 360 to 590 nm possibly because of the presence of a small amount of impurity in which there is not a redox active MV^{2+}.

(16) (a) Yonemoto, E. H.; Saupe, G. B.; Schmehl, R. H.; Hubig, S. M.; Riley, R. L.; Iverson, B. L.; Mallouk, T. E. *J. Am. Chem. Soc.* **1994**, *116*, 4786. (b) Yonemoto, E. H.; Riley, R. L.; Kim, Y. I.; Atherton, S. J.; Schmehl, R. H.; Mallouk, T. E. *J. Am. Chem. Soc.* **1992**, *114*, 8081.

(17) (a) Excited state potentials were calculated from the free energy content of the excited state above the ground state, ΔG^0_{ES}, by $\Delta G^0_{ES} = \lambda_{O,L} + E_o$. E_o is the $\upsilon^* = 0 \rightarrow \upsilon = 0$ energy gap and $\lambda_{O,L}$ the solvent reorganizational energy including low-frequency modes treated classically. They were determined by emission spectra fitting techniques described elsewhere (refs 17b,c). (b) Claude, J. P.; Meyer, T. J. *J. Phys. Chem.* **1995**, *99*, 51. (c) Kober, E. M.; Caspar, J. V.; Lumpkin. R. S.; Meyer, T. J. *J. Phys. Chem.* **1986**, *90*, 3722.

(18) (a) As estimated from $\lambda = 4k_BT \ln(k_BT/hk_{ET})$ with $k_{ex} = k_{ET}K_A$, where K_A is the association constant (ref 18b). With $k_{ex} = 2.2 \times 10^9$ M^{-1} s^{-1} for 10-(CH$_3$)PTZ$^{+/0}$ (ref 18c) and $K_A \sim 0.69$ M^{-1} (ref 18e), $\lambda = 0.78$ eV. Given $k_{ex} = 8.4 \times 10^6$ M^{-1} s^{-1} for MV$^{2+/+}$ (ref 18d), $\lambda = {}^1/_2(\lambda_{11} + \lambda_{22}) \sim 0.90$ eV for $k_{ET.}$ (b) Marcus, R. A.; Sutin, N. *Biochim. Biophys. Acta* **1985**, *811*, 265. (c) Kowert, B. A.; Marcoux, L.; Bard, A. J. *J. Am. Chem. Soc.* **1972**, *94*, 5538. (d) Bock, C. R.; Connor, J. A.; Gutierrez, A. R.; Meyer, T. J.; Whitten, D. G.; Sullivan, B. P.; Nagle, J. K. *Chem. Phys. Lett.* **1979**, *61*, 252. (e) From the Eigen-Fuoss equation (refs 18b,f,g), $K_A = (4\pi N d^3/3000)\cdot\exp(-w_r/RT)$ with $w_r = (z_Az_Be^2)/(D_Sd(1 + \beta d\sqrt{\mu}))$ and $\beta = ((8\pi Ne^2)/(1000D_Sk_BT))^{1/2}$. The separation distance $d_{PTZ} = r_{PTZ} + r_{PTZ^+} \sim 6.5$ Å, and $d_{MV} = r_{MV^{2+}} + r_{MV^+} \sim 3.3$ Å. Radii were calculated by using the formula $r = {}^1/_2(d_xd_yd_z)^{1/3}$, in which d_x, d_y, d_z are the lengths of the three molecular axes. (f) Eigen, M. *Z. J. Phys. Chem. (Munich)* **1954**, *1*, 176. (g) Fuoss, R. M. *J. Am. Chem. Soc.* **1958**, *80*, 5059.

(19) Molecular mechanics optimization utilized a MM2 force field. The initial positions were determined by rotating around the bond between the 4-carbon and the benzylic carbon until the $-\mathrm{MV}^{2+}$ and $-\mathrm{PTZ}$ were in close proximity. The distances are quoted as the separations between the geometric centers of the redox pairs.